Interface adjustment and exchange coupling in the IrMn/NiFe system

F. Spizzo[1], M. Tamisari [1], F. Chinni[1], E. Bonfiglioli[1] and L. Del Bianco[1]

[1] *Dipartimento di Fisica e Scienze della Terra and CNISM, Università di Ferrara, I-44122 Ferrara, Italy*

Corresponding authors: F. Spizzo (e-mail: federico.spizzo@unife.it);

L. Del Bianco (e-mail: lucia.delbianco@unife.it)

Abstract

The exchange bias effect was investigated, in the 5-300 K temperature range, in samples of IrMn[100Å]/NiFe[50Å] (set A) and in samples with inverted layer-stacking sequence (set B), produced at room temperature by DC magnetron sputtering in a static magnetic field of 400 Oe. The samples of each set differ for the nominal thickness (t_{Cu}) of a Cu spacer, grown at the interface between the antiferromagnetic and ferromagnetic layers, which was varied between 0 and 2 Å. It has been found out that the Cu insertion reduces the values of the exchange field and of the coercivity and can also affect their thermal evolution, depending on the stack configuration. Indeed, the latter also determines a peculiar variation of the exchange bias properties with time, shown and discussed with reference to the samples without Cu of the two sets. The results have been explained considering that, in this system, the exchange coupling mechanism is ruled by the glassy magnetic behavior of the IrMn spins located at the interface with the NiFe layer. Varying the stack configuration and t_{Cu} results in an adjustment of the structural and magnetic features of the interface, which ultimately affects the spins dynamics of the glassy IrMn interfacial component.

Keywords: magnetic exchange coupling, interface adjustment, glassy magnetic behavior, magnetic correlation length, Cu spacer

Highlights:

Exchange bias effect in IrMn/NiFe samples with interfacial Cu spacer

A variation of exchange bias with time is observed in as-deposited samples

Magnetic variation of the interface by varying the stack sequence and Cu thickness

Interface adjustment affects the dynamics of interfacial IrMn spins

The exchange bias properties can be tuned by interface adjustment

1. Introduction

A main requirement for the technological application of giant or tunneling magnetoresistive devices, as read-heads or in magnetic random access memories (MRAMs), is to achieve a fine control of the magnetization reversal process in the ferromagnetic (FM) electrodes [1]. To this aim, the most commonly used method is coupling the FM layer to an antiferromagnetic (AFM) one by magnetic exchange interaction [2], so as to give rise to an unidirectional anisotropy for the FM spins (exchange anisotropy) because of the torque action exerted on them by the AFM spins. As a consequence, a horizontal shift of the hysteresis loop of the AFM/FM system is experienced (exchange bias, EB, effect expressed by the exchange field parameter H_{ex}) [3, 4], which is almost invariably accompanied by a coercivity (H_C) enhancement [5, 6]. Hence, it is well established that the effective magnetic anisotropy of the FM layer can be tailored by acting on several parameters, such as the AFM magnetic anisotropy and the FM and AFM layer thickness [3]. Regarding the origin of the EB phenomenon, some articles contributed to the controversial debate about that reporting about exchange biasing through a non-magnetic spacer at the AFM/FM interface, thus suggesting that this can be a good method to tune the strength of the exchange coupling. [7, 8, 9, 10, 11]. Indeed, Several models have been proposed for the exchange coupling mechanism and some of them assign a crucial role to the magnetic stability of the AFM nanograins, generally assumed as non-interacting [11, 12, 13]. A similar description was also used to account for the increase of H_{ex} with time observed in IrMn/CoFe samples subjected to He ion bombardment that alters the structure and the anisotropy of the AFM component [14].

Recent studies have demonstrated the existence of AFM regions with spin-glass like magnetic properties at the interface with the FM phase, originating from the concomitance of structural disorder and existence of competing magnetic interactions as a consequence of the lack of structural periodicity [13, 15, 16]. In particular, we coherently explained the EB properties of IrMn/NiFe samples, in form both of continuous films and of dot arrays, considering the glassy magnetic behavior of a structurally disordered IrMn region located between the FM phase and the ‘bulk’ of

the AFM layer, clearly detected by high-resolution transmission electron microscopy analyses [17, 18]. The glassy magnetic nature of these AFM regions implies a complex magnetic dynamics of AFM spins, governed by intertwined parameters such as temperature, anisotropy energy barriers distribution and length of magnetic correlation [19, 20, 18, 21]. In this context, in this research work, we will show that it is possible tuning the EB properties of IrMn/NiFe samples, i.e. H_{ex}, H_C and their thermal dependence, by adjusting the AFM/FM interface, namely its position in the layer-stacking sequence and its extension, through the insertions of Cu islands. The results are explained considering that this interface modulation ultimately affects the magnetic dynamics of the glassy AFM component.

2. Experimental

Samples deposition was carried out at room temperature by DC magnetron sputtering in a 2 mTorr Ar atmosphere, in a static magnetic field H_{dep} = 400 Oe. The FM and AFM phases were $Ni_{80}Fe_{20}$ (NiFe) and $Ir_{25}Mn_{75}$ (IrMn), respectively. The films were grown on a naturally oxidized Si substrate, covered by a 5nm-thick Cu underlayer to favor crystalline order and texture and thus enhance the EB effect [22, 23]. We prepared two sets of samples differing for the stack sequence: i) set A, with structure Si/Cu(50 Å)/IrMn(100 Å)/Cu(t_{Cu})/NiFe(50 Å), where t_{Cu}, the nominal thickness of the Cu layer, was 0, 0.5, 1, 2 Å; ii) set B with structure Si/Cu(50 Å)/ NiFe(50 Å)/Cu(t_{Cu})/IrMn(100 Å), with t_{Cu} = 0, 1 and 2 Å. Hence, in set A the FM layer is grown at the top of the stack whereas it is at the bottom in set B, apart from the Cu underlayer. With reference to the set and to t_{Cu}, the samples were labeled with the general notation *set_nameCu-*t_{Cu}.

The magnetic properties were investigated by measuring hysteresis loops at temperature T in the 5-300 K range, using both a superconducting quantum interference device (SQUID) magnetometer and a longitudinal magneto-optic Kerr effect (MOKE) apparatus with the polarization modulation technique. SQUID and MOKE measurements were carried out on all the samples immediately after deposition. In the as-deposited state at T = 300 K, all the samples appeared substantially saturated

(in no sample the difference between the remanent magnetization and the saturation magnetization exceeded 10 %) and horizontally shifted by exchange anisotropy. Then, the samples were stored at room temperature in a vacuum of ~ 10^{-3} mbar and their magnetic properties at T = 300 K were checked by MOKE during about one year. At the end of this aging period, SQUID measurements were performed again on all the samples and no variation in their magnetic moment at saturation was detected. This is a hint that no oxidation took place during the aging period, but it is to be expected that oxygen passivation occurred when the samples were extracted from the deposition chamber.

3. Results and discussion

3.1 Magnetic structure of the interface in samples with no Cu

In this section, we describe the EB properties of samples ACu-0 and BCu-0, namely belonging to sets A and B respectively and without Cu spacer. Fig. 1a shows a typical hysteresis loop shifted by exchange anisotropy (in particular, it has been measured at T = 300 K on the as-deposited ACu-0 sample). We define the exchange field H_{ex} and the coercivity H_C as positive parameters in this way: $H_{ex} = -(H_{right}+H_{left})/2$ and $H_C = (H_{right}-H_{left})/2$, H_{right} and H_{left} being the points where the loop intersects the field axis.

In Fig. 1b, H_{ex} and H_C measured at T = 300 K in sample ACu-0 as-deposited (time = 0 days) and during a period of 300 days are reported. A marked increase in H_{ex}, passing from ~140 Oe to ~ 285 Oe is experienced during the first 42 days of aging; after 300 days the total variation of H_{ex} amounts to ~ 124%. During the whole period, H_C undergoes just a very small decrease and the final value is ~ 100 Oe. In Fig. 2a, the thermal dependence of H_{ex} and H_C is shown for the sample aged 2 and 300 days. The difference in the values of H_{ex} reduces more and more with decreasing T below 300 K and is negligible at the lowest temperature. Irrespective of aging, H_{ex} and H_C decrease with increasing T, especially in the 5-100 K range, as revealed by the analysis of the derivative curves

(Fig. 2c). This thermal evolution of the two parameters was already observed in IrMn/NiFe bilayers, independently of the position of the NiFe layer in the stack, and it was explained through a simplified model based on the existence of a structurally and magnetically disordered IrMn region interposed between the FM phase and the 'bulk' of the AFM layer [17, 18]. The latter was found to consist of nanograins [18], supposed magnetically independent or just weakly interacting. It is worth recalling the main conclusions descending from such a description. Two different magnetic regimes characterize the magnetothermal behavior of the IrMn/NiFe system. At T = 5 K, the interfacial IrMn spins are frozen in a long-range correlated glassy magnetic state and collectively involved in the exchange coupling with the NiFe spins, which results in a maximized EB effect. At T = 5 K, H_{ex} ~860 Oe in ACu-0; the high value of H_C (~ 530 Oe), in comparison with that of a single 5nm-thick NiFe reference film (~20 Oe), reveals the presence of AFM spins, which are dragged by the FM ones during the magnetization reversal (often indicated as rotatable spins in literature [[24]]), probably because of a lower local anisotropy within the frozen state. With increasing T above 5 K, thermal effects reduce the length of magnetic correlation among interfacial AFM spins as well as their effective anisotropy [25], leading to a marked decrease in both H_{ex} and H_C. T = 100 K can be schematically indicated as the temperature where the collective frozen state of the interfacial AFM component breaks up, resulting in a collection of spins magnetically uncorrelated (or correlated on a very short length, i.e. small clusters). In this regime, only the AFM interfacial spins that, under the polarizing action of the bulk AFM spins, are tightly anchored to the AFM nanograins may have an effective anisotropy strong enough to produce the EB effect. Hence, for T > 100 K, the thermal dependence of H_{ex} is determined by the strength of the polarizing action of the bulk AFM nanograins on the interfacial spins and by their thermal stability. No exchange coupling can be observed when the AFM nanograins definitely enter the superparamagnetic regime.

The analysis of EB properties on sample BCu-0 gives the results shown in Fig. 2b: at T = 300 K, the increase in H_{ex} after aging is just ~ 10% (basically, the full variation was seen to occur within 5 days since the deposition) and, also in this sample, such a difference lessens with decreasing T; the

thermal dependence of H_C is not modified by the sample aging. After aging, H_{ex} and H_C in the two samples differ for an amount that at no temperature exceeds 80 Oe (basically, the largest values are measured in ACu-0).

Although the presence of the magnetic field H_{dep} during the deposition of sample ACu-0 may favor a certain preferential orientation of the AFM spins, their configuration cannot minimize the interface exchange energy with the FM spins, simply because the NiFe layer is grown after the IrMn one. At T = 300 K, the marked increase of H_{ex} with time (Fig. 1b) can be explained considering that the AFM spins undergo a thermally-activated magnetic relaxation process towards a lower energy configuration, resulting in a much stronger exchange coupling at the AFM/FM interface. To support this explanation, we verified that no variation of H_{ex} with time occurred in a sample perfectly similar to ACu-0, but put in liquid nitrogen soon after deposition and kept at T ~ 80 K for the following two weeks. After this period, the sample was removed from liquid nitrogen, kept at room temperature and analyzed by MOKE at regular time intervals during the subsequent 30 days: H_{ex} was found to increase with time, essentially reproducing the behavior shown in Fig. 1b.

It may be assumed that this relaxation process involves just the interfacial AFM spins, which ultimately rule the interface exchange coupling mechanism. Indeed, regarding this effect, to discriminate between interface AFM spins and bulk AFM nanograins is extremely difficult from the experimental point of view, but it also appears quite speculative from the conceptual point of view. In fact, we assume that at T = 300 K the interfacial spins effectively involved in the exchange coupling mechanism are just those that are strongly anchored to the spin lattice of the bulk AFM nanograins. Therefore, the magnetic relaxation of the interfacial AFM component necessarily involves to a certain extent also the bulk AFM nanograins and vice-versa.

Passing to sample BCu-0, when the FM layer is grown first, H_{dep} is largely sufficient to reach its magnetic saturation; thus, the AFM spins are forced to assume a minimum energy configuration already during the deposition process. Therefore, soon after deposition, at T = 300 K, H_{ex} is much

higher in BCu-0 compared to ACu-0 (~ 235 Oe and ~ 140 Oe, respectively) and just a small (~10%) increase of H_{ex} with time is observed (Fig. 2b).

It is noteworthy that neither in ACu-0 nor in BCu-0 any variation of H_{ex} with time is experienced at the lowest temperature (Fig. 2a,b), namely in correspondence to the collective frozen regime of interfacial AFM spins. This indicates that, irrespective of the configuration assumed by interfacial AFM spins at T = 300 K with aging, when the temperature approaches T = 100 K and is further lowered, they always freeze in a configuration energetically equivalent to that assumed in the as-deposited state, resulting in the same macroscopic magnetic anisotropy and, hence, in the same exchange coupling strength.

3.2 Interface adjustment by Cu spacer insertion

In this Section, we report exclusively the magnetic properties measured on samples of sets A and B after a period not shorter than three months since the deposition. Since the nominal values of t_{Cu} are lower than the Cu lattice parameter (3.61 Å), obviously the Cu layer cannot be continuous. It is to be expected that Cu islands formed at the IrMn/NiFe interface, their total volume increasing more and more with increasing t_{Cu}. It is worth remarking that the values of magnetic moment per unit area measured in the samples of each set are consistent within an experimental error of 7% (the average value is ~ 3.3×10^{-4} emu/cm^2 in set A and just slightly lower in set B; no correlation exists between the deviations from the average values and t_{Cu}). Hence, no significant Cu diffusion takes place in the NiFe layer and, presumably, in the IrMn one neither. In support to this statement, one should also consider that the sputtering process was carried out at room temperature and that we avoided subsequent field-cooling procedures from high temperature to trigger the EB effect.

The curves of H_{ex} and H_C vs. T for the two set of samples are shown in Fig. 3 (including those for ACu-0 and BCu-0, already displayed in Fig. 2). The general trend of the curves is quite similar – in particular, they all show the marked rising tendency for T < 100 K - but, at each temperature, H_{ex}

and H_C decrease with increasing t_{Cu}. This result certainly reflects the reduction of the spatial extension of the IrMn/NiFe interface due to the insertion of Cu islands. We have also verified that a sample of type A with t_{Cu} = 4 Å shows, at T = 300 K, the same H_{ex} (~ 35 Oe) found in ACu-2, whereas no hint of exchange coupling is observed in a sample with t_{Cu} = 8 Å. This supports the idea that the Cu islands grow also in thickness before the full in-plane coverage is accomplished.

However, if the effect of the Cu spacer insertion was only 'geometrical', i.e. the presence of Cu islands just reduces the extension of the IrMn/NiFe interface area, and both the EB properties of the samples and their magnetothermal evolution are not affected by that, the curves of H_{ex} vs. T, in Fig. 3a and 3b, should overlap once normalized to their value at T = 5 K, so as to indicate a similar thermal dependence of H_{ex} in all the samples.

To facilitate such a comparison, the normalized curves are shown in Fig. 4. The curves for set B are substantially superposed (Fig. 4b). On the contrary, regarding set A, they are nearly coincident only for ACu-0 and ACu-0.5, whereas in ACu-1 and especially in ACu-2 a much more pronounced thermal dependence is observed (Fig. 4a), especially in the 5-100 K range. Very similar trends are obtained considering H_C instead of H_{ex}, namely normalizing the H_C vs. T curves of Fig. 3c and 3d (not shown).

Hence, the growth of the Cu spacer leads to quite different behaviors in sets A and B and, in the first case, it substantially alters the thermal dependence of H_{ex} and H_C. We propose that the explanation is connected with the different type of structural and, hence, magnetic modulation of the interface, obtained through the insertion of the Cu islands in the two cases. The stack configuration for samples A and B can be schematically depicted as shown in Fig. 5. The relevant feature is that in samples A the structurally disordered glassy magnetic component of the AFM layer is homogenously spread throughout the extension of the IrMn/NiFe interface, whereas it is not in samples B. This difference affects the way in which the interfacial AFM spins are magnetically correlated. In fact, in samples A, a full magnetic correlation of AFM interfacial spins can be achieved at the lowest temperature since, in principle, the correlation length can become infinite

(Fig. 5a). In the B-type configuration, the Cu islands constitute structural constraints that hamper the magnetic correlation (Fig. 5b). Accordingly, in samples B, the AFM interfacial spins actively involved in the exchange coupling mechanism are those that directly face the FM layer. All of them 'feel' the interaction with the NiFe spins and, in the low-temperature frozen regime, they assume a configuration that fulfills both the requirement of minimizing the exchange coupling with the NiFe spins, on one side, and with the blocked spins of the bulk AFM nanograins, on the other side.

On the contrary, in samples A, the AFM interfacial spins directly facing the FM layer are also magnetically correlated with those facing the Cu islands, which feel the interaction with the bulk AFM nanograins, but not the interaction with the NiFe spins. In this case, also the AFM interfacial spins not directly facing the FM layer do determine the final frozen configuration of the glassy AFM component and, therefore, play a role in the exchange coupling mechanism.

Actually, it is interesting to note that this different aspect of the interface in samples A and B ultimately does not affect the values of H_{ex} and H_C measured at T = 5 K (Fig. 3), i.e. when the length of magnetic correlation reaches its maximum extension, as depicted in Fig.5a and 5b.

This indicates that, despite the energy minimum in which the AFM interfacial spins get locked at T = 5 K may be different in samples A and B, the macroscopic magnetic anisotropy of the frozen AFM component is comparable, due to the inherent magnetic stiffness of the fully frozen collective regime.

However, with increasing temperature, the magnetic length correlating the AFM interfacial spins reduces, approaching and then becoming shorter than the Cu islands interdistance. We propose that the consequences of the interface modulation become more and more relevant with rising temperature in samples A (the case is depicted in Fig. 5c). In fact, with increasing T or, for a fixed T, with increasing t_{Cu} namely the extension of the Cu islands, within a region of magnetically correlated AFM interfacial spins, the fraction of those facing the Cu islands (subjected just to the exchange interaction with the bulk AFM nanograins) increases. As a consequence, all the AFM

interfacial spins inside a correlated region tend to better fulfill the requirement of minimizing the exchange energy with the spins of the bulk AFM nanograins, which leads to a reduction of H_{ex} more pronounced than expected for the mere decrease of the IrMn/NiFe interface extension, consistently with the results in Fig. 4a. Moreover, since in samples with larger t_{Cu} the AFM interfacial spins are more strongly anchored to the bulk AFM nanograins, a strong reduction of H_C is also experienced (Fig. 3c), because the tendency of interfacial AFM spins to follow the FM ones during reversal is more firmly opposed.

On the contrary, things do not change substantially in samples B, as suggested by the sketches in Fig. 5b and 5d, apart from the fact that in Fig. 5d, due to the higher temperature, the effective anisotropy of interfacial AFM spins must be assumed inherently lower than in Fig. 5b: at all temperatures, the Cu islands just act so as to reduce the NiFe/IrMn interface extension. This affects H_{ex} more and more with increasing t_{Cu} (Fig. 3b) and, to a lesser extent, also H_C (Fig. 3d), but not their thermal dependence (Fig. 4b).

An important achievement of this study, in the perspective of technological applications, it that it is possible to tune the values of H_{ex} and H_C to a good extent, as well as their thermal dependence, by changing t_{Cu} and the stack configuration. To highlight this conclusion, in Fig. 6 we compare the loops measured at T =300 K on (a) samples ACu-0 and ACu-2 and (b) samples BCu-0 and BCu-2. It is noteworthy that H_C ~1 Oe in ACu- 2 and BCu-2 – namely, the samples are as soft as the reference NiFe film at the same temperature – but the loops are clearly shifted, being H_{ex} ~30 Oe in ACu-2 and as large as ~110 Oe in BCu-2.

Conclusions

The EB effect has been studied in two sets of IrMn/NiFe samples differing for the layer-stacking sequence and characterized by the presence of an interface Cu spacer. The nominal thickness t_{Cu} of such a spacer was varied between 0 and 2 Å, necessarily resulting in the formation of Cu islands at

the interface between the AFM and FM layers . In the samples with no Cu, the evolution of the EB properties with temperature and time has been coherently explained by refining a previous description [17, 18] and, hence, considering that interfacial AFM spins exhibit a glassy magnetic behavior and that their relaxation dynamics, driven by the exchange coupling with the FM spins, depends on the relative position of the AFM and FM layers in the stack.

In the samples with Cu spacer, the values of H_{ex} and H_C decrease with increasing t_{Cu}. However, the thermal dependence of H_{ex} and H_C is not modified by the Cu spacer in the case of samples of set B, whereas it is significantly altered in samples of set A. The results have been explained considering that the growth of the Cu islands reduces the extension of the IrMn/NiFe interface, but a different modulation of the interface structure is obtained with changing the stacking sequence, actually. In particular, such a different modulation affects the length of magnetic correlation of interfacial AFM spins and, consequently, the exchange coupling mechanism. Indeed, modulating the interface by varying t_{Cu} and the stack sequence provides a valuable tool to tune H_{ex}, H_C as well as their thermal dependence.

Acknowledgments

This research work was sponsored by MIUR under project FIRB2010 ‘Tailoring the magnetic anisotropy of nanostructures for enhancing the magnetic stability of magnetoresistive devices - NANOREST’

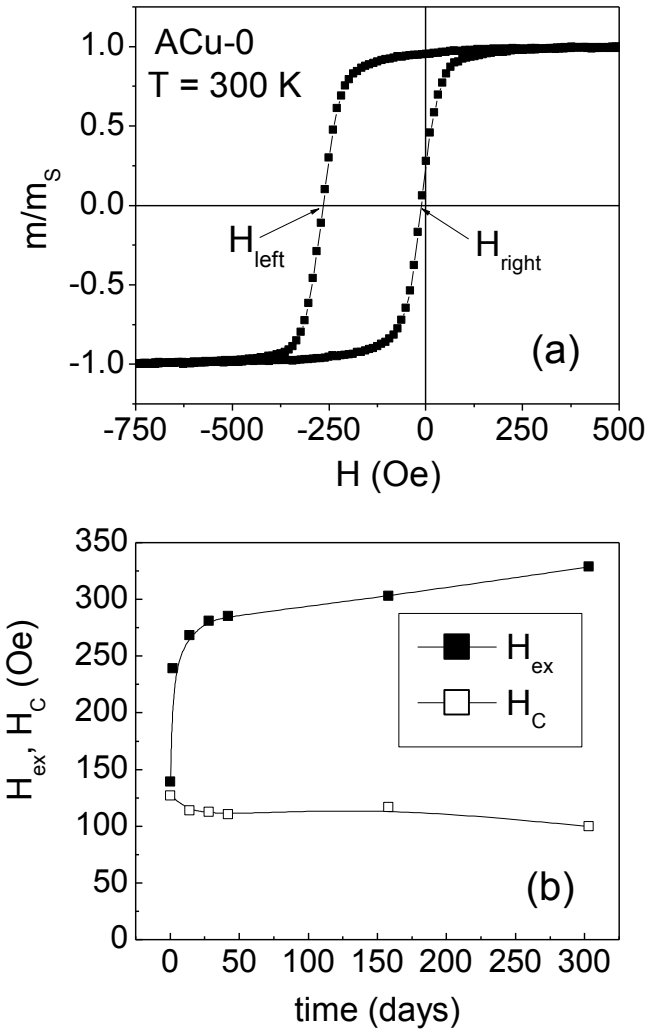

Figure 1. (a) Hysteresis loop measured at T = 300 K on sample ACu-0 as-deposited (normalized to the magnetic moment at saturation m_S). (b) Evolution of the exchange field H_{ex} (full symbols) and of the coercivity H_C (open symbols) with time in sample ACu-0, measured at T = 300 K. Time = 0 corresponds to the day of deposition of the film by DC magnetron sputtering. The error bars are smaller or comparable to the size of the dots. Solid lines are guides to the eye

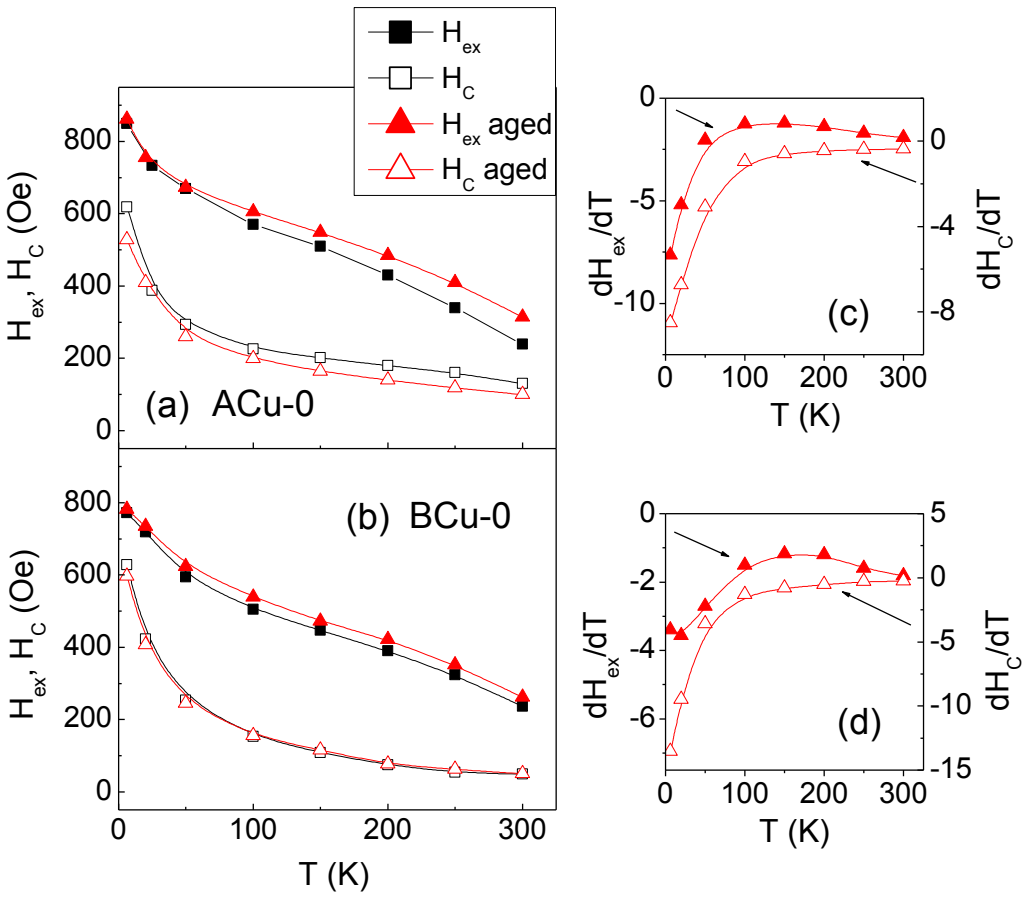

Figure 2. (color online) H_{ex} and H_C as a function of temperature T measured in (a) sample ACu-0 and (b) sample BCu-0, within the first 48 hours since the deposition (squares) and after 300 days (triangles); more precisely, ACu-0 was measured after two days since the deposition and BCu-0 in the very same day of the deposition. The small frames on the right show the derivatives curves dH_{ex}/dT and dH_C/dT relative to the samples aged for 300 days: (c) sample AuCo-0; (d) sample BCu-0.

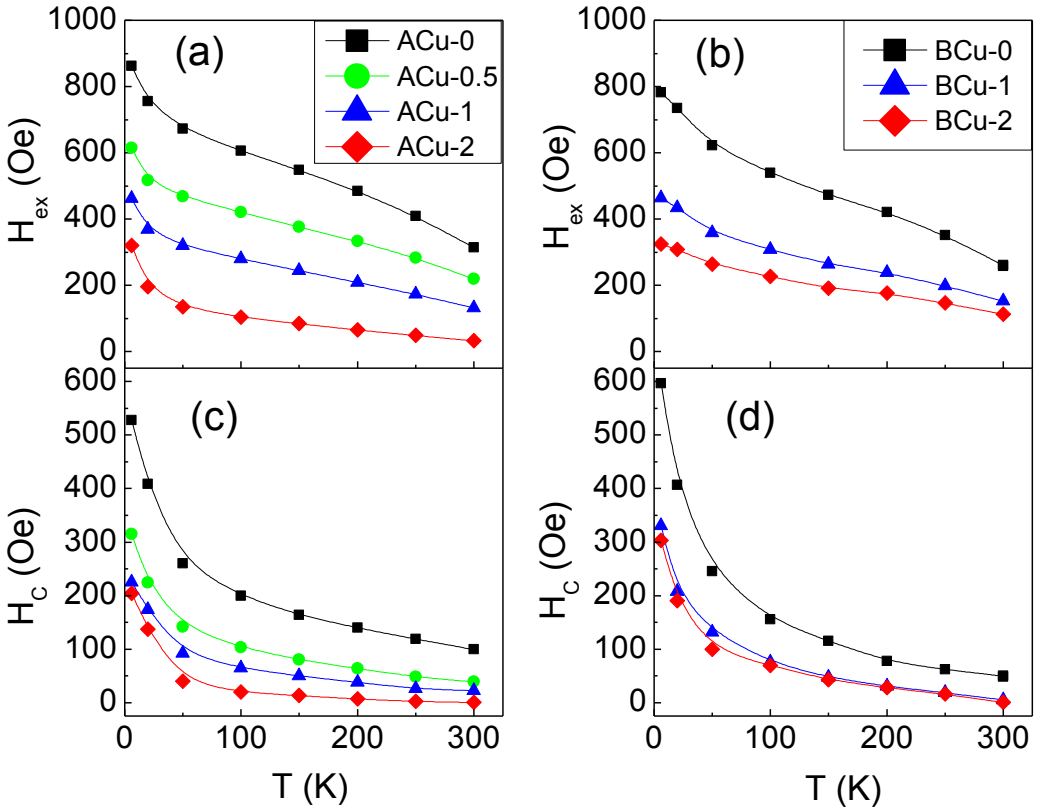

Figure 3. (color online) (a) H_{ex} vs. T for samples of set A (NiFe layer at the top of the stack sequence); (b) H_{ex} vs. T for samples of set B (NiFe layer at the bottom of the stack sequence); (c) H_C vs. T for set A samples; (d) H_C vs. T for set B samples.

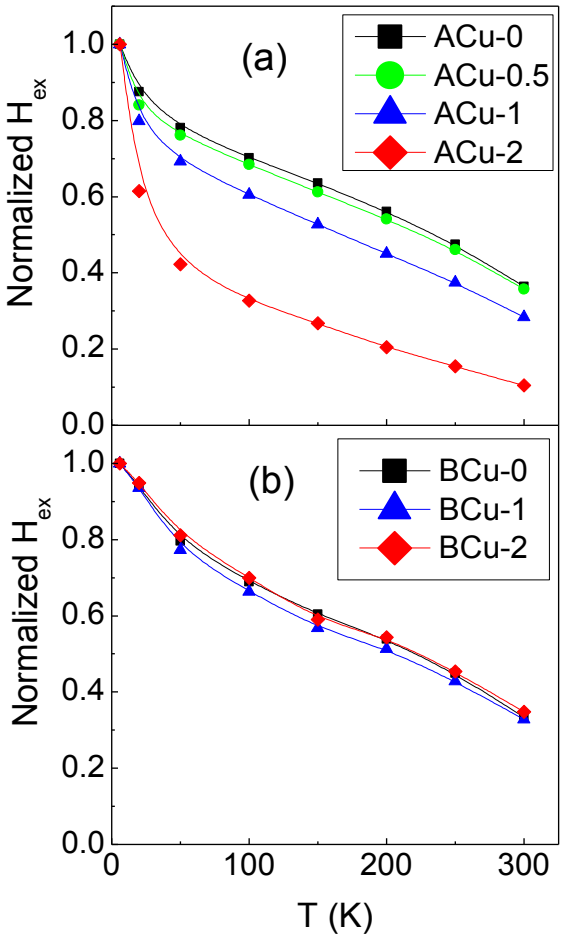

Figure 4. (color online) H_{ex} vs. T curves of (a) set A samples and (b) set B samples, shown as normalized to the values of H_{ex} at T = 5 K.

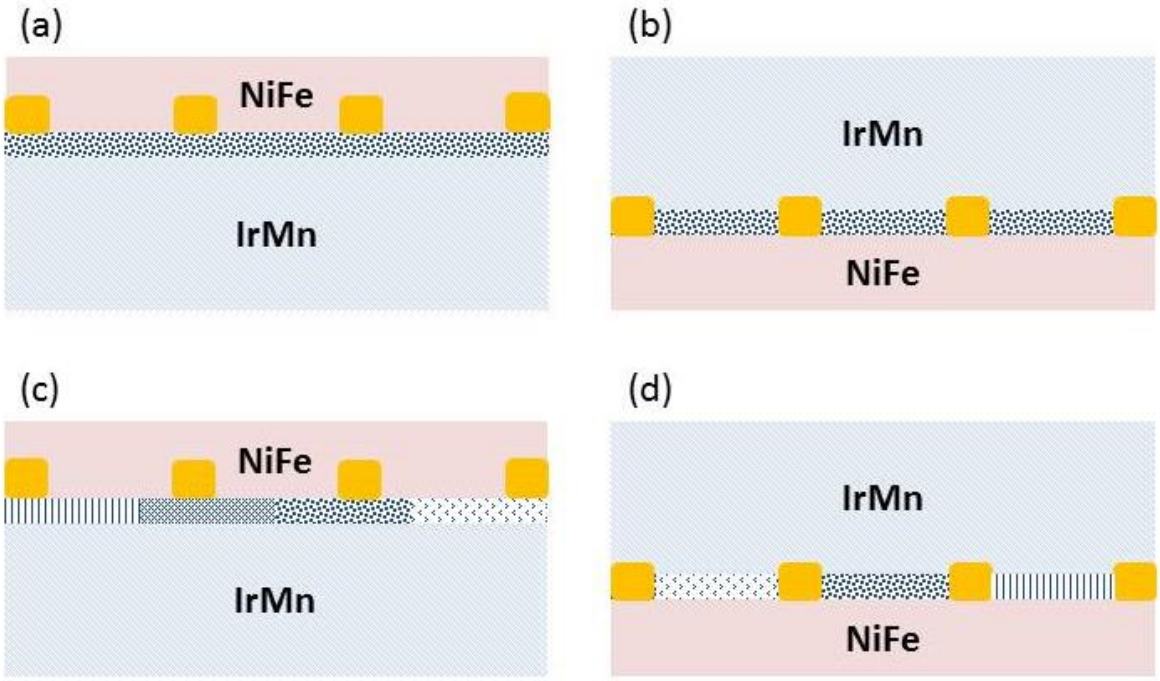

Figure 5. (color online) Schematic pictures of the structure of samples with Cu islands (rectangles) at the interface between the IrMn and NiFe layers. Sketches (a) and (c) depict a type-A sample, whereas (b) and (d) are relative to a type-B sample. In (a) and (b), the dotted regions represent the interfacial disordered IrMn component, showing a glassy magnetic behavior. The same graphical motif is used to identify such a component, to suggest the idea that both the situations are assumed occur at the lowest temperature T = 5 K: in (a), the magnetic correlation among the interfacial IrMn spins reaches the largest extension; in (b) the magnetic correlation is hampered by the Cu islands. In sketches (c) and (d), different graphical motifs are used to represent the glassy IrMn component, to suggest the existence of several regions of magnetically correlated IrMn interfacial spins: this is expected to occur when the temperature is raised above T = 5 K and the magnetic correlation length shortens. See text for further explanation.

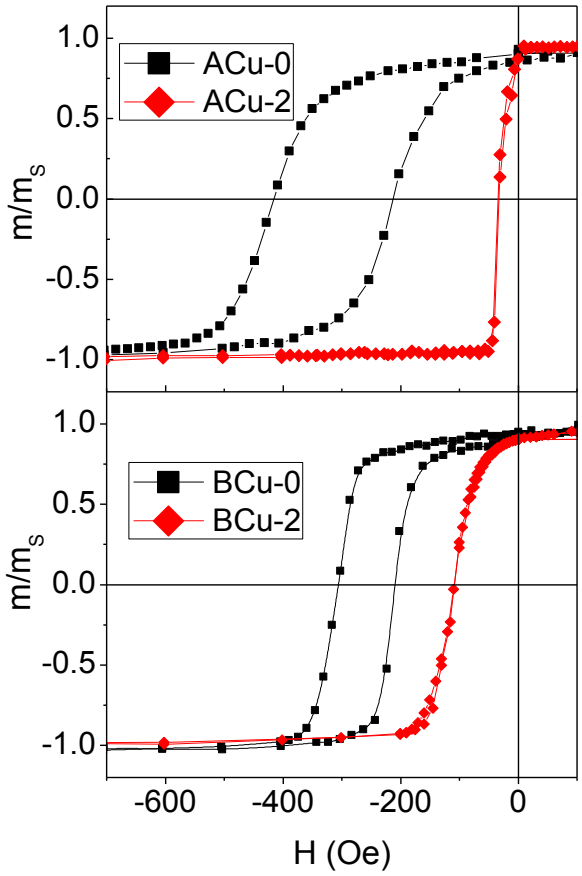

Figure 6. (color online) Hysteresis loops measured at T = 300 K in samples ACu-0 and ACu-2 (a) and in samples BCu-0 and BCu-2 (b). The loops are relative to the aged samples; they are normalized to the magnetic moment at saturation m_S.

References

[1] C. Chappert, A. Fert, F.N.V. Dau, The emergence of spin electronics in data storage, *Nature Mater*., 6, (2007) 813. DOI: 10.1038/nmat2024

[2] B. Dieny, V.S. Speriosu, S.S.P. Parkin, B.A. Gurney, D.R. Wilhoit, D. Mauri, Giant magnetoresistive in soft ferromagnetic multilayers, Phys. Rev. B 43 (1991)1297. DOI: 10.1103/PhysRevB.43.1297

[3] W.H. Meiklejohn, C.P. Bean, Phys. Rev. 102 (5) (1956) 1413.

[4] J. Nogués, J. Sort, V. Langlais, V. Skumryev, S. Suriñach, J.S. Muñoz, M.D. Barò, Exchange bias in nanostructures, Phys. Rep. 422 (2005) 65. DOI: 10.1016/j.physrep.2005.08.004

[5] D. V. Dimitrov, Shufeng Zhang, J. Q. Xiao, G. C. Hadjipanayis, and C. Prados, Effect of exchange interactions at antiferromagnetic/ferromagnetic interfaces on exchange bias and coercivity, Phys. Rev. B 58 (1998) 12090. DOI: 10.1103/PhysRevB.58.12090

[6] S. Laureti, L. Del Bianco, B. Detlefs, E. Agostinelli, V. Foglietti, D. Peddis, A. M. Testa, G. Varvaro, and D. Fiorani, Interface exchange coupling in a CoPt/NiO bilayer, Thin Solid Films 543 (2013) 162. DOI: 10.1016/j.tsf.2012.12.115

[7] L. Thomas, A. J. Kellock, S. S. P. Parkin, On the exchange biasing through a nonmagnetic spacer layer, J. Appl. Phys. 87 (2000) 5061. DOI:10.1063/1.373248

[8] Y.-G. Yoo, S.-G. Min, S.-C. Yu, Influence of spacer layer in exchange coupled NiFe/Cu/IrMn trilayer structure, J. Magn. Magn. Mater. 304 (2006) e718. DOI: 10.1016/j.jmmm.2006.02.201

[9] J. Wang, W. N. Wang, X. Chen, H. W. Zhao, J. G. Zhao, W. Sh. Zhan, The effect of the interlayer on the exchange bias in FeMn/Cu/Co system, J. Appl. Phys. 91 (2002) 7236. DOI: 10.1063/1.1447872

[10] J. Geshev, T. Dias, S. Nicolodi, R. Cichelero, A. Harres, J. J. S. Acuña, L. G. Pereira, J. E. Schmidt, C. Deranlot, F. Petroff, Role of the uncompensated interface spins in polycrystalline

exchange-biased systems, J. Phys. D: Appl. Phys. 44 (2011) 095002. DOI:10.1088/0022-3727/44/9/095002

[11] J. Geshev, S. Nicolodi, L. G. Pereira, L. C. C. M. Nagamine, J. E. Schmidt, C. Deranlot, F. Petroff, R. L. Rodríguez-Suárez, A. Azevedo, Exchange bias through a Cu interlayer in an IrMn/Co system, Phys. Rev. B 75 (2007) 214402. DOI: 10.1103/PhysRevB.75.214402

[12] G. Vallejo-Fernandez, T. Deakin, K. O'Grady, S. Oh, Q. Leng, and M. Pakala, J. Appl. Phys. **107**, 09D709 (2010)

[13] V. Baltz, B. Rodmacq, A. Zarefy, L. Lechevallier, B. Dieny, Bimodal distribution of blocking temperature in exchange-biased ferromagnetic/antiferromagnetic bilayers, Phys. Rev. B 81 (2010) 052404. DOI: 10.1103/PhysRevB.81.052404

[14] A. Ehresmann, C. Schmidt, T. Weis, and D. Engel, Thermal exchange bias field drift in field cooled $Mn_{83}Ir_{17}$ / $Co_{70}Fe_{30}$ thin films after 10 keV He ion bombardment, J. Appl. Phys. 109 (2011) 023910. DOI: 10.1063/1.3532046

[15] J. McCord, S. Mangin, Separation of low- and high-temperature contributions to the exchange bias in $Ni_{81}Fe_{19}$-NiO thin films, Phys. Rev. B 88 (2013) 014416. DOI:10.1103/PhysRevB.88.014416

[16] L. Del Bianco, F. Boscherini, M. Tamisari, F. Spizzo, M. Vittori Antisari, E. Piscopiello, Exchange bias and interface structure in the Ni/NiO nanogranular system, J. Phys. D: Appl. Phys. 41 (2008) 134008. DOI: 10.1088/0022-3727/41/13/134008

[17] F. Spizzo, M. Tamisari, E. Bonfiglioli, L. Del Bianco, Detection of the dynamic magnetic behavior of the antiferromagnet in exchange-coupled NiFe/IrMn bilayers, J. Phys. Cond. Matt. 25 (2013) 386001. DOI: 10.1088/0953-8984/25/38/386001

[18] F. Spizzo, E. Bonfiglioli, M. Tamisari, A. Gerardino, G. Barucca, A. Notargiacomo, F. Chinni, L. Del Bianco, Magnetic exchange coupling in IrMn/NiFe nanostructures: from the continuous film to dot arrays, Phys. Rev. B. 91 (2015) 064410. DOI: 10.1103/PhysRevB.91.064410

[19] V. Baltz, G Gaudin, P. Somani, B. Dieny, Influence of edges on the exchange bias properties of ferromagnetic/antiferromagnetic nanodots, Appl. Phys. Lett. 96 (2010) 262505. DOI: 10.1063/1.3449123

[20] R. Carpenter, A. J. Vick, A. Hirohata, G. Vallejo-Fernandez and K. O'Grady, Effect of grain cutting in exchange biased nanostructures, J. Appl. Phys. 115 (2014) 17B905. DOI: 10.1063/1.4868328

[21] F. Spizzo, M. Tamisari, F. Chinni, E. Bonfiglioli, A. Gerardino, G. Barucca, D. Bisero, S. Fin, L. Del Bianco, Exchange bias properties of 140nm-sized dipolarly interacting circular dots with ultrafine IrMn and NiFe layers, J. Magn. Magn. Mater. 400 (2016) 242 DOI: 10.1016/j.jmmm.2015.08.001

[22] M. Pakala, Y. Huai, G. Anderson, L. Miloslavsky, Effect of underlayer roughness, grain size, and crystal texture on exchange coupled IrMn/CoFe thin films, J. Appl. Phys. 87 (2000) 6653. DOI: 10.1063/1.372800

[23] M. Tsunoda, K. Imakita, JMMM 304 (2006) 55

[24] H. Ohldag, A. Scholl, F. Nolting, E. Arenholz, S. Maat, A. T. Young, M. Carey, and J. Stöhr, Phys. Rev. Lett. **91**, 017203 (2003)

[25] J. A. Mydosh in *Spin glasses: an experimental introduction*, edited by Taylor and Francis (London 1993)